Study of the influence of charge carrier traps on the linearity of a CCD photodetector

© V.V. Sidorov[1,2], P.V. Petrov[2]

[1] V.G. Khlopin Radium Institute
194021 St. Petersburg, Russia
[2] Ioffe Institute,
194021 St. Petersburg, Russia

E-mail: pavel.petrov@gmail.com

Received November 7, 2024
Revised November 22, 2024
Accepted November 22, 2024

We study the properties of a silicon CCD photodetector using the lock-in technique. At low illumination intensities, nonlinearity of the photodetector characteristics is detected due to the presence of traps in the charge accumulation zone. A theoretical model is developed that allows one to describe the experimental results and calculate the concentration and energy of the traps. It is demonstrated that using the energy and concentration of the traps as calibration coefficients, it is possible to linearize the results of CCD photodetector measurements.

Keywords: CCD photosensor, charge carrier traps, electro-neutrality equation, lock-in technique.

DOI: 10.61011/SC.2024.11.59960.7299

1. Introduction

Charge-coupled devices (CCDs), such as CCD matrices and linear arrays, are widely used as photodetectors in modern laboratories. Their main advantage is a high quantum yield, as well as the possibility of simultaneous multichannel recording of signals from individual sections of the matrix — the so-called pixels. At the same time, CCD detectors also have certain disadvantages. One such shortcomings that prevents operation with weak signals is the presence of $1/f$ noise inherent in many semiconductor devices. The usual way of improving the signal-to-noise ratio is to accumulate many frames from the photodetector, with their subsequent averaging. The presence of $1/f$ noise in the photodetector signal leads to the fact that after accumulating a certain number of frames, further averaging does not lead to an improvement in the signal-to-noise ratio. This greatly limits the ability of CCD photodetectors to work with weak signals, the measurement of which is necessary, for example, in spectral studies of single quantum objects, such as localized excitons [1,2]. In addition to noise, another typical challenge facing CCD photodetectors when working with weak signals is non-zero dark currents, which is a separate complex issue to consider [3].

The traditional way to overcome the above-mentioned measurement problems is by using a lock-in technique. Widely applied in single-channel photodetectors, it has not been widely used in CCD photodetectors because of the difficulties encountered in demodulating large amounts of data from multiple pixels. In this paper, we were able to resolve this technical issue by creating high-performance software that enables real-time demodulation of the signal from 2048 pixels of a CCD photodetector. Measurements using the synchronous detection technique allowed measuring the CCD photodetector signal in the low illumination intensity mode. The study of the signal dependence on pumping intensity revealed the presence of a nonlinear section in the weak intensity mode associated with the presence of traps in the charge accumulation zone. A comparison of the measurement results with a theoretical model constructed by solving the electroneutrality equation allowed us to estimate the number and bond energy of traps for each pixel. Using these data as calibration coefficients allowed pixel-by-pixel linearization of the CCD photodetector characteristic.

2. Experimental setup

In this paper, we studied the performance of a commercially available Thorlabs LC100 CCD camera based on a Sony ILX554B CCD chip. This device is a linear array of 2048 56 $\times$ 14 micron pixels. Compared to other devices used in optical spectroscopy, the Thorlabs LC100 camera has a relatively high recording speed reaching 900 frames per second. This property makes it convenient for working with modulated signals.

The diagram of the measurement setup is shown in Figure 1. A light-emitting diode was used to illuminate the camera, the radiation intensity of which was modulated by the so-called analog-to-digital modulation. The radiation amplitude was a sequence of rectangular pulses, the amplitude of which was modulated in a sinusoidal manner. At the moment of the pulse, a charge is accumulated in the photodetector, while in the interval between pulses the result is read. Such modulation is necessary because the Sony ILX554B CCD chip does not have a shutter and reading must take place in the dark. The duration of one pulse was 1.054 ms. The time dependences of the signals of analog, digital and analog-to-digital modulation are shown

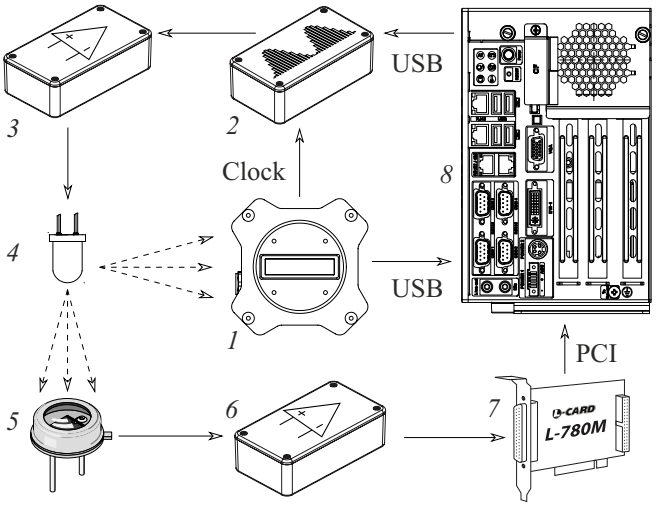

Figure 1. Schematic diagram of the experimental setup: *1* — Thorlabs LC100 CCD camera, *2* — modulator, *3* — LED driver, *4* — LED, *5* — photodiode, *6* — photodiode signal amplifier, *7* — ADC, *8* — computer.

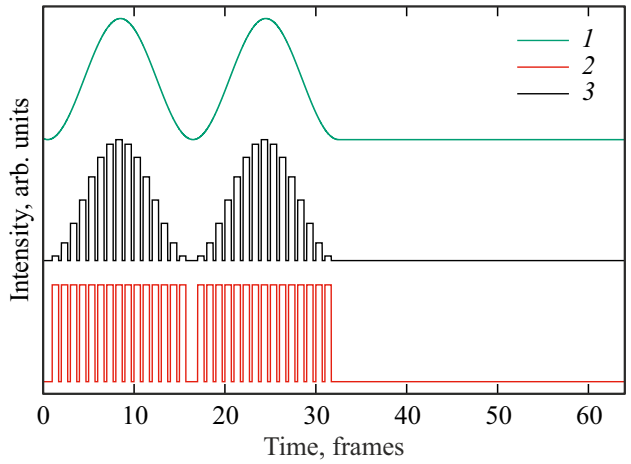

Figure 2. Analog (*1*), digital (*2*) and analogue-to-digital (*3*) modulation signal versus time. Two modulation periods are shown followed by a zero section necessary for measuring the dark signal.

in Figure 2. Since the source of the synchronization signal was a Thorlabs LC100 CCD camera, direct transmission of the modulation phase was technically impossible. Therefore, the measured signal from each pixel of the CCD photodetector was processed by means of the so-called quadrature demodulation, which allows obtaining the amplitude of the measured signal S according to the following formulas:

$$A = \frac{2}{NM} \sum_{i=0}^{N-1} \sum_{j=0}^{M-1} S_{(M\cdot i+j)} \sin 2\pi \frac{j}{M},$$

$$B = \frac{2}{NM} \sum_{i=0}^{N-1} \sum_{j=0}^{M-1} S_{(M\cdot i+j)} \cos 2\pi \frac{j}{M},$$

$$S = \sqrt{A^2 + B^2}.$$

Here M is the number of frames per modulation period, N is the number of periods in a series of measurements, S_i is the signal of the i-th measurement. When processed using this method, the result will consist of a signal at the modulation frequency and the Fourier component of the recording system noise at the same frequency. In order to subtract the noise component, a dark signal was measured (Figure 2), which was also demodulated and then subtracted from the signal of the illuminated photodetector.

Independent of the CCD photodetector, the emission intensity was monitored by a BPW20RF silicon photodiode, the signal from which was amplified by a low-noise, zero-drift LTC2057HV operational amplifier. The amplified signal was recorded by the Lcard L-780M ADC, and the measurement results were demodulated using the same scheme as the signal from the CCD camera. Blue, red, and green LEDs were used for pumping. No qualitative difference was observed for illumination with different wavelengths; the paper provides the results obtained with blue LED illumination.

3. Photon transfer curve

To accurately calibrate the CCD-photodetector readings, we measured the so-called „photon transfer curve“. The idea behind this technique is to measure the dependence of the signal variance on the mean signal of the photodetector. There is usually a linear plot on this dependence. The availability of such an area means that the photodetector at such signal intensities is linear and the noise is fluctuation noise by nature. Indeed, in the fluctuation noise mode, the mean signal depends on the number of photons in direct proportion to N, and root-mean-square deviation — as $\sqrt{N}$. Then the mean square is also proportional to N. The inverse slope of this line is simply the number of photoexcited electrons in units of e^- per one ADC sample [4]. The photon transfer curve measurements were performed according to the method typical for such measurements [5]. The CCD photodetector was uniformly illuminated by the LED light. At a given illumination intensity of the CCD matrix, a series of N frames were sequentially sampled. For each i-th pixel mean signal $\overline{S_i}$ and its variance were calculated. σ_i^2:

$$\overline{S_i} = \frac{1}{N} \sum_{1}^{N} S_i; \quad \sigma_i^2 = \overline{S_i^2} - \overline{S_i}^2.$$

The obtained values $\overline{S_i}$ and σ_i^2 were averaged over all pixels.

The measured photon transfer curve shown in Figure 3 consists of three sections. In the range from 2000 to 8000 ADC samples the curve is linear, which indicates that the photodetector is linear in this range. From the slope of the straight line the photon transfer coefficient was determined, which for the investigated photodetector was equal to $K = 75.7\, e^-/$ (ADC count) of photoelectrons per one count of the analogue-to-digital converter (ADC).

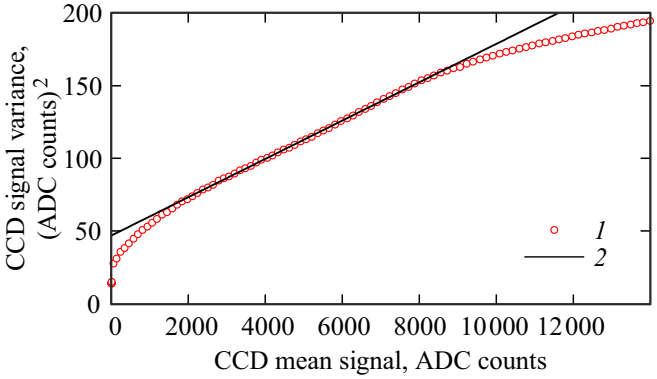

Figure 3. Photon transfer curve: *1* — measurement result, *2* — least-squares linear fit.

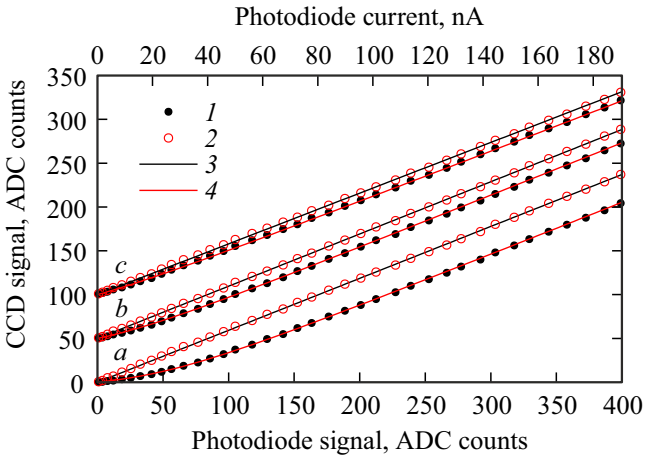

Figure 4. The CCD photodetector signal versus illumination intensity for three pixels: large (*a*), intermediate (*b*), and small (*c*) degrees of nonlinearity, shifted along the ordinate axis for clarity. The figure shows: *1* — measured dependence of the CCD photodetector signal on the photodiode current, *2* — the linearised CCD photodetector signal recalculated by eq. (4), *3* — the result of least-squares fitting by the $y = ax$, *4* — fitting of the measurement results by eq. (2).

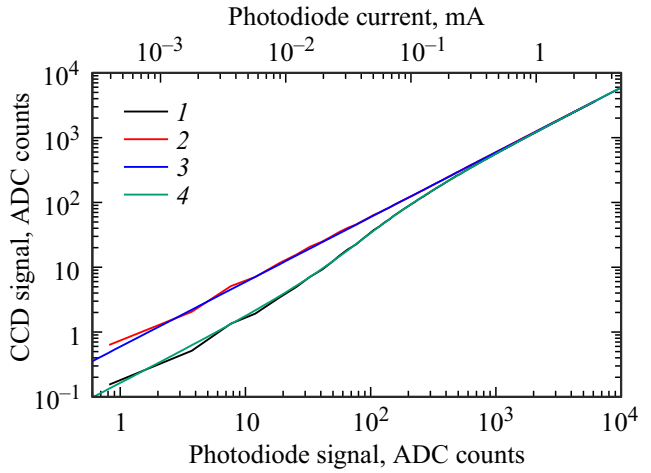

Figure 5. CCD photodetector signal versus illumination intensity in double logarithmic scale for a pixel with a large degree of nonlinearity. Designations are the same as in Figure 4.

Deviations of the curve from linearity are observed at high and low signals. Nonlinearity at high signals is usually associated with overflow of the potential well for electrons during charge accumulation and, thus, is inherent in all CCD photodetectors. Usually, it does not create problems during measurements, since an excessively strong signal can be easily weakened with a light filter. In this paper, we will study the nonlinearity that manifests itself in the low-light mode.

4. Results of CCD photodetector linearity measurements

Figure 4 shows the results of measurements of the dependence of the CCD-photodetector signal on the illumination intensity, taken in the lock-in detection mode. It can be seen that at low illumination the signal grows non-linearly, whereas at high illumination it comes to a linear dependence passing through a point just below the origin. For the sake of illustration, the measurement results from only three pixels are presented: with small, intermediate and large degree of nonlinearity. The most natural explanation for the nonlinear nature of the dependence is the presence of traps in the charge accumulation zone. Some of the photoexcited electrons are localized on the traps and do not contribute to the measured signal. As the pumping increases and the number of photoexcited electrons becomes much larger than the number of traps, the dependence of the signal on pumping becomes linear. To illustrate the behaviour of the photodetector at high illuminations, Figure 5 shows the results of measurements plotted in double logarithmic scale. The transition to a linear dependence at signals of the order of 1000 ADC bits is clearly visible, which agrees with the results of measurements of the photon transfer characteristic (Figure 3).

5. Theoretical model

To verify the proposed hypothesis about the influence of traps on the photodetector linearity, we considered a theoretical model based on the electroneutrality equation [6]. Assuming that the energy level of the traps is far from the edge of the conduction band at energy E_t much more than kT, we will use the approximation of Boltzmann statistics. Considering the charge accumulation zone as unalloyed, only the concentration of photoexcited holes Δp equal to the total concentration of photoexcited electrons Δn the concentration of photoexcited electrons located in the conduction band and contributing to the signal $n = N_a \exp(E_f/kT)$, as well as a summand for electrons localised on traps, which we assume to be neutral, should be included in the electroneutrality equation. Neglecting the presence of background donors and acceptors, the electroneutrality equation can be written as follows:

$$N_c A + \frac{N_t}{A^{-1}\exp(-E_t/kT) + 1} = \Delta p; \quad A = \exp\frac{E_f}{kT}. \quad (1)$$

Here E_f is a quasi-Fermi level for electrons, N_t is trap concentration, $N_c = 2.86 \cdot 10^{19}\,\mathrm{cm}^{-3}$ is the effective density of states in silicon at room temperature [7]. Strictly speaking, the term corresponding to the electron concentration on traps should contain in the denominator a pre-exponential factor depending on the degeneracy factor of the state. Since for deep traps in silicon this parameter is usually unknown, for simplicity it is assumed that this factor is equal to 1. Equation (1) is a quadratic equation in the coefficient A and can be easily solved. Then the charge concentration in the conduction band can be written as $n = N_c A$:

$$n = \frac{1}{2}\left(\Delta p - a + \sqrt{(\Delta p - a)^2 + b\Delta p}\right), \qquad (2)$$

where the following notations are introduced for convenience

$$a = N_t + N_c \exp\left(-\frac{E_t}{kT}\right);$$

$$b = 4N_c \exp\left(-\frac{E_t}{kT}\right). \qquad (3)$$

The plus sign before the square root in expression (2) is chosen from the physical considerations that in the limit of high optical pumping, most of the traps should be filled and then the concentration of free electrons will be equal to $n = \Delta p - N_t$. It is easy to see that this is true by decomposing the summand containing the square root into a power series in the limit of large Δp. Figure 3 shows the result of fitting the experimental curve by equation (2) using the coefficients a and b as fitting parameters. The fitting was performed using the Nelder-Mead optimization algorithm [8]. The use of the coefficients a and b as calibration coefficients allowed us to perform a pixel-by-pixel linearisation of the CCD photodetector measurements using the formula

$$\Delta n = \Delta p = \frac{4n(n+a)}{4n+b}. \qquad (4)$$

The eq. (4) is easy to obtain by expressing Δp from eq. (2). The result of linearization using eq. (4) is shown in Figures 4 and 5. It is evident that the use of the developed technique allows for ensuring the linearity of the photodetector for the dynamic range $\sim 10^4$. Using (3), it is easy to obtain formulas for the surface concentration of traps N_t, as well as for the average localization energy of traps E_t:

$$N_t = K\,\frac{a - b/4}{14\mu \times 56\mu}, \qquad (5)$$

$$E_t = kT \ln\left(N_c^{-2/3}\,\frac{Kb}{14\mu \times 56\mu}\right). \qquad (6)$$

For computational convenience, the parameters a, b, n, Δn and Δp were measured in ADC bits of the CCD photodetector. Therefore, to switch to surface concentrations, they must be multiplied by K and divided by the pixel area. The eqs. (5)–(6) were used to estimate the values

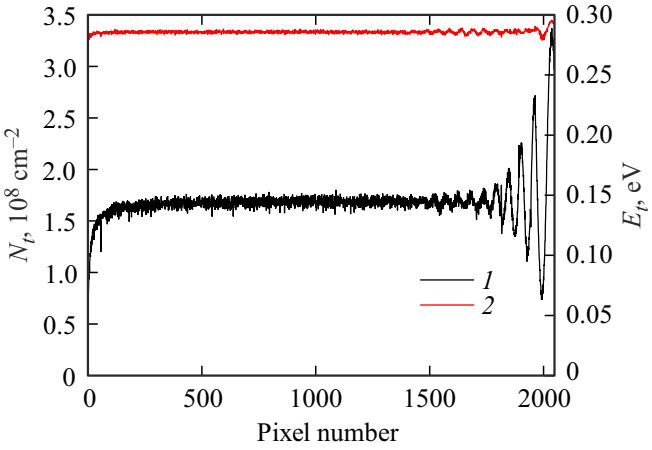

Figure 6. Dependences of the surface concentration N_t (*1*) and trap energies E_t (*2*) on the photodetector pixel number.

of surface concentration and trap localisation energy in each pixel of the photodetector, shown in Figure 6. The average surface concentration of traps is relatively small and is $1.7 \cdot 10^8\,\mathrm{cm}^{-2}$ indicating good photodetector quality. The energy level of traps is ~ 0.3 eV. A number of papers have been found in the scientific literature in which traps with similar localisation energy [9–12] have been observed in silicon-based structures. The most common interpretation is that they are not due to the presence of any particular impurity, but correspond to either vacancy complexes or substitution defects.

The oscillations of the surface concentration of traps observed on one side of the CCD matrix look unusual. It would seem that the trap concentration should not vary significantly along the sample surface, much less oscillate. However, the occurrence of oscillations can be easily explained by the influence of large-scale fluctuations of the electrostatic potential arising from the photodetector electronics operation. The energy levels of defect-related traps generally have some finite width. In the absence of illumination, the Fermi level must lie somewhere inside the widened trap level partially filled with electrons. In this case, if in some section of the CCD the electrostatic potential shifts the trap level downward relative to the Fermi level, the fraction of traps filled with electrons will increase, which will result in a local decrease in the concentration of empty traps. On the contrary, an increase in the potential will result in more empty traps locally.

To validate this assumption, the dependences of the electronic Fermi quasi-level position on n were plotted using the eq. (7) for three pixels: with large, intermediate, and small observed trap concentrations (Figure 7):

$$E_f = kT \ln\left(N_c^{-2/3}\,\frac{Kn}{14\mu \times 56\mu}\right). \qquad (7)$$

At high light levels, the Fermi quasi-level positions for all three pixels match well and are approximately equal to $-E_t/2$. This corresponds to the situation when all traps are

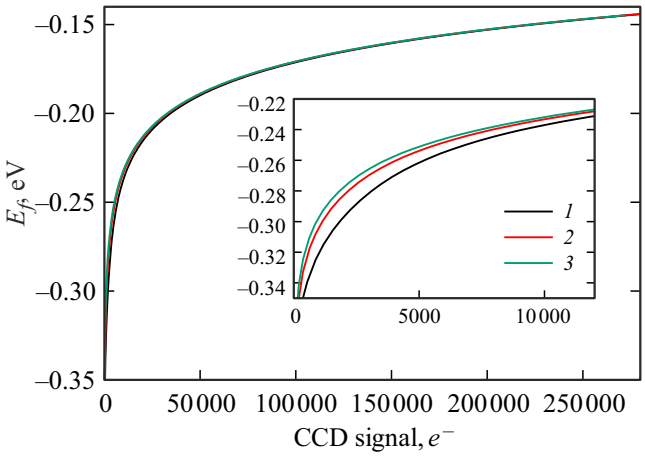

Figure 7. Dependence of the Fermi quasi-level position E_f on the number of photoexcited electrons Δn for three pixels: with high (*1*), intermediate (*2*), and low (*3*) trap concentrations. The inset shows a low-light area in the enlarged scale.

filled and the behavior of the pixels is the same. At low light levels, the quasi-Fermi level for pixels with a high trap concentration is located lower by energy ~ 10 meV. The mean E_t values in pixels with high and low trap concentrations differ by approximately the same energy, confirming our assumption.

6. Conclusion

In this paper, the properties of a photodetector based on a CCD matrix are analysed by means of the lock-in detection method. The non-linearity of the light characteristic at low illumination intensities is explained by the presence of traps in the charge accumulation zone. The theoretical model developed allowed us to estimate the number and energy of trap localisation and to linearise the measurement results.

Funding

This study was supported by grant No. 23-22-00333 from the Russian Science Foundation.

Conflict of interest

The authors declare that they have no conflict of interest.

References

[1] A.S. Gritchenko, I.Y. Eremchev, A.V. Naumov, P.N. Melentiev, V.I. Balykin. Opt. Laser Techn., **143**, 107301 (2021).
[2] P.V. Petrov, I.A. Kokurin, G.V. Klimko, S.V. Ivanov, Yu.L. Ivánov, P.M. Koenraad, A.Yu. Silov, N.S. Averkiev. Phys. Rev. B, **94**, 115307 (2016).
[3] A.B. Zakharov, M.E. Prokhorov, M.S. Tuchin, A.V. Evenko, A.O. Zhukov, A.I. Gladyshev, N.I. Shakhov, Y.G. Kharlamov, N.A. Zhukova. Oboronnyi kompleks — nauchny.-techn. progresu Rossii, vyp. 1, 43 (2019). (in Russian).
[4] J.R. Janesick. *Photon Transfer* (SPIE Press Monograph, 2007) v. PM 170.
[5] S.E. Bohndiek, A. Blue, A.T. Clark, M.L. Prydderch, R. Turchetta, G.J. Royle, R.D. Speller. IEEE Sensors J., **8** (10), 1734 (2008).
[6] A.I. Ansel'm. *Vvedenie v teoriyu poluprovodnikov* (M., Nauka, 1978). (in Russian).
[7] M.A. Green. J. Appl. Phys., **67** (6), 2944 (1990).
[8] P.K. Mogensen, A.N. Riseth. J. Open Source Software, **3** (24), 615 (2018).
[9] E.V. Astrova, V.B. Voronkov, V.A. Kozlov, A.A. Lebedev. Semicond. Sci. Technol., **13** (5), 488 (1998).
[10] P. Lévêque, P. Pellegrino, A. Hallén, B. Svensson, V. Privitera. Nucl. Instrum. Meth. Phys. Res. Section B: Beam Interactions with Materials and Atoms, **174** (3), 297 (2001).
[11] I.E. Tyschenko, V.P. Popov, P.A. Dementyev. FTP, **45** (3), 335 (2011). (in Russian).
[12] Ye.V. Ivanova, M.V. Zamoryanskaya, FTT, **61** (8), 1448 (2019). (in Russian).

Translated by J.Savelyeva